Growth-coupled reverse β-oxidation enables redox-balanced fatty-alcohol fermentation and strain evolution

Bridgie Cawthon[1,2 †], Aidan E. Cowan[1 † *], Zen Yoshikawa[1,2], Kenneth Low[1], Justin Baerwald[1,2], Matthew Incha[1,3], Jennifer Gin[1], Yan Chen[1], Christopher J. Petzold[1], Edward E. K. Baidoo[1], Emine A. Turumtay[1], Adam M. Feist[1,4,5], Jay D. Keasling[1,2,5,6,7 *]

[†]Denotes equal contribution, names ordered alphabetically

*Corresponding authors aidancowan@berkeley.edu, keasling@berkeley.edu

[1]Joint BioEnergy Institute, Lawrence Berkeley National Laboratory, Emeryville, CA 94608, USA
[2]Department of Chemical and Biomolecular Engineering, University of California, Berkeley, Berkeley, CA 94720, USA
[3]Department of Bioresource and Environmental Security, Sandia National Laboratories, Livermore, CA 94551, USA
[4]Department of Bioengineering, University of California, San Diego, CA, USA
[5]The Novo Nordisk Foundation Center for Biosustainability, Technical University of Denmark, Kemitorvet, Building 220, Kongens Lyngby 2800, Denmark
[6]QB3 Institute, University of California, Berkeley, Berkeley, CA 94720, USA
[7]Department of Bioengineering, University of California, Berkeley, Berkeley, CA 94720, USA

Supplementary Table 1: Strains used in this study

Strain name	Genotype	Description	Registry #	Reference
CM15	E. coli MG1655 Δ*araBAD* Δ*fadRE* Δ*ldhA* Δ*ackApta* Δ*adhE* Δ*poxB* Δ*frdABCD*	Fermentation-deficient strain used as a base for complementation by rBOX expression	JBx_109929	[1]
CM15-TFA	CM15 **pSeva_TER_ACR** and **pBbA6a_fadAB**	Fermentation-deficient strain containing plasmid **pSeva_TER_ACR** and **pBbA6a_fadAB**	JBx_277738	This study
CM15-TA	CM15 **pSeva_TER_ACR**	Fermentation-deficient strain containing plasmid **pSeva_TER_ACR**	JBx_277739	This study
CM15-F	CM15 **pBbA6a_fadAB**	Fermentation-deficient strain containing plasmid **pBbA6a_fadAB**	JBx_277740	This study
CM15-TFA$_{EnRx}$	See Fig. 4 for genomic characterization.	Evolved CM15-TFA strain. Independent evolution replicate n from round x of ALE.		This study
CM15-TFA$_{E2R18}$	CM15-TFA *leuS* R502S *opgH* S523P *atoC* I129S TRC -10 T>C	Evolved CM15-TFA strain determined to be fastest growing and further characterized in bioreactor fermentations.	JBx_277741	This study
BL21 (DE3) FadA WT	BL21 (DE3) **pet28a_FadA_WT**	Expression strain containing plasmid **pet28a_FadA_WT**	JBx_277742	This study
BL21 (DE3) FadA Q59K	BL21 (DE3) **pet28a_FadA_Q59K**	Expression strain containing plasmid **pet28a_FadA_Q59K**	JBx_277743	This study
XL1-Blue	*E. coli* XL1-blue (*rec*A1 *end*A1 *gyr*A96 *thi*-1 *hsd*R17 *sup*E44 *rel*A1 lac [F′ *proAB lacI*^{q}ZΔ*M15* Tn*10* (Tet r)])	Used for DNA storage and preparation		Commercially available (Agilent)

Plasmid names are bolded

Supplementary Table 2: Plasmids used in this study

Plasmid name	Description	Registry #	Reference
pSeva_TER_ACR	Expression construct for *trans*-2-enoyl-CoA reductase (TER) from *Treponema denticola* and acyl-CoA reductase (ACR) from *Marinobacter aquaeolei* under control of the trc promoter	JBx_277729	This study
pBbA6a_fadAB	Expression construct for 3-ketoacyl-CoA thiolase (FadA) and Fatty acid oxidation complex subunit alpha (FadB) from *E. coli* under control of the LlacO-1 promoter.	JBx_277733	This study
pet28a_FadA_WT	Expression construct for 3-ketoacyl-CoA thiolase (FadA)	JBx_277735	This study
pet28a_FadA_Q59K	Expression construct for 3-ketoacyl-CoA thiolase (FadA) with Q59K substitution	JBx_277737	This study

Supplementary Table 3: Primers used in this study

Primer	Sequence
BC1	5'– cggtgtttgagcgggtttaaggatccaaactcgagtaagg –3'
BC2	5'– gtcgcctttgtaaagcatatgtatatctccttcttaaaagatcttttga –3'
BC3	5'– atccttactcgagtttggatccttaaacccgctcaaacacc –3'
BC4	5'– cttttaagaaggagatatacatatgctttacaaaggcgacac –3'
BC5	5'– atgcgtgggatttactggtaagactcctgttgatagatcca –3'
BC6	5'– ccattcgatggtgtcgacgtcggccgcgaattccagaaatc –3'
BC7	5'– agcgctttgaccgtatctaagcgtgtgtgaatcgcagaaa –3'
BC8	5'– ttaccagtaaatcccacgca –3'

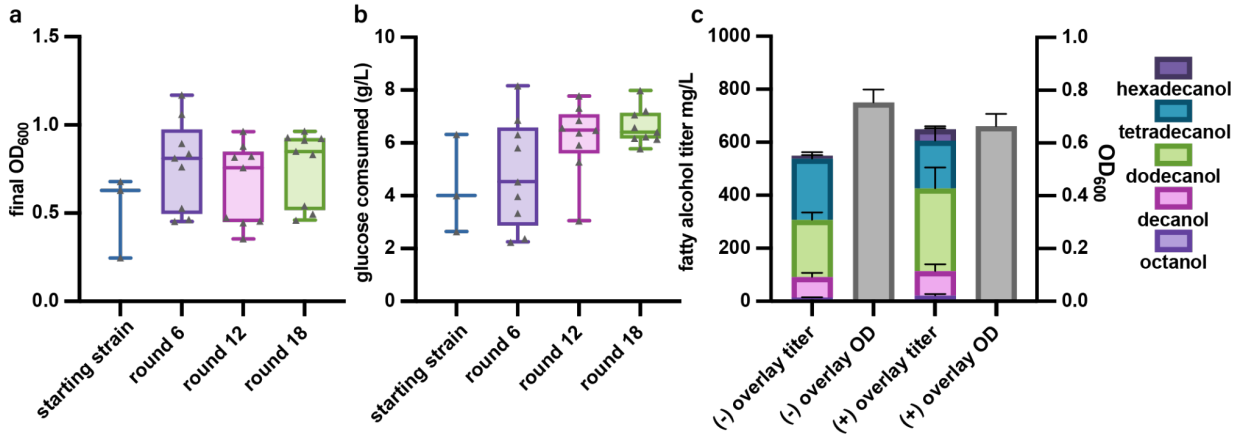

Supplementary Figure 1 Final optical density and titer of cultures tested from ALE
a, Final optical density of isolates from round 6, 12, and 18 of ALE (n=9) compared to the starting CM15-TFA strain (n=3). **b,** Glucose consumed in each culture of isolates from round 6, 12, and 18 of ALE (starting concentration 20 g/L) (n=9) compared to the starting CM15-TFA strain (n=3). **c,** Fatty-alcohol titer and final OD achieved in small-scale cultures of CM15-TFA$_{E2R18}$ with (+) and without (-) 20% (v/v) dodecane overlay. All differences are not statistically significant.

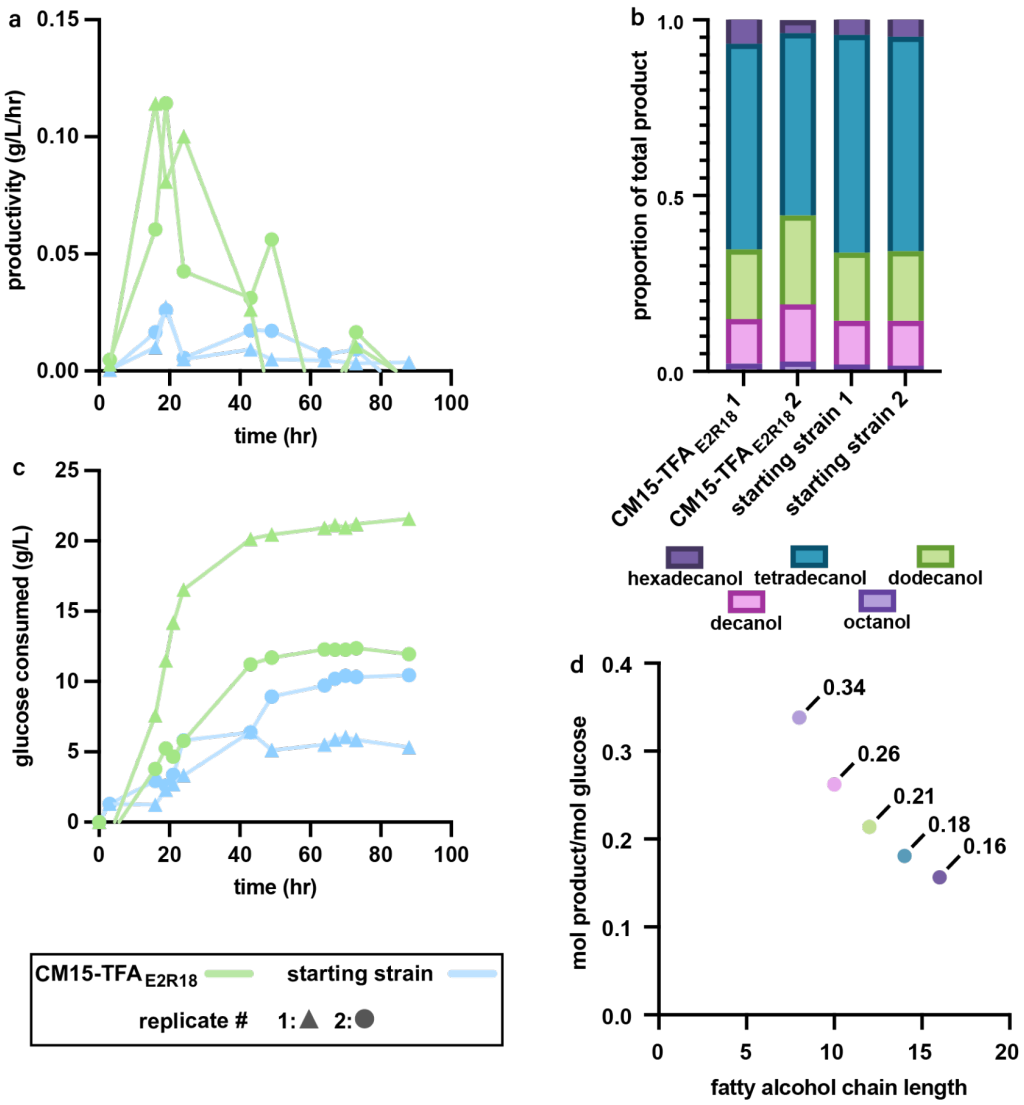

Supplementary Fig. 2 Bioreactor fatty-alcohol production by the starting strain CM15-TFA and evolved strain CM15-TFA$_{E2R18}$

a, Time course of fatty-alcohol productivity for bioreactors inoculated with either starting strain (CM15-TFA) or CM15-TFA$_{E2R18}$. **b,** For each bioreactor, fatty-alcohol composition is shown as the molar fraction of total fatty-alcohol titer contributed by each chain-length species. **c,** Glucose consumed over the course of fermentation in each bioreactor. **d,** Predicted molar production of assayed fatty alcohols per mol glucose. Theoretical yield predictions were generated by metabolic modeling using flux balance analysis.

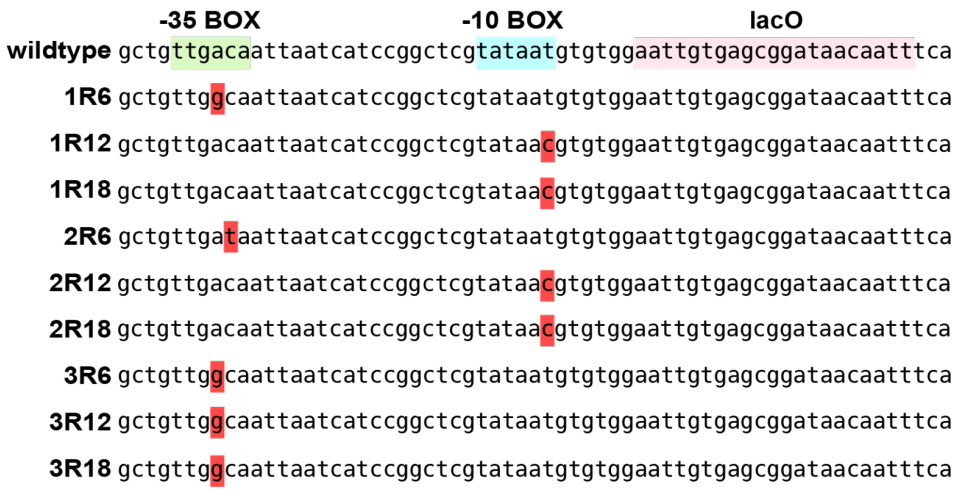

Supplementary Figure 3 Mutations to TRC promoter of pSEVA_TER_ACR

Mutations to the TRC promoter of pSEVA_TER_ACR are highlighted in red for each sequenced isolate from the ALE experiment. All mutations are located in either the -35 or -10 BOX of the TRC promoter.

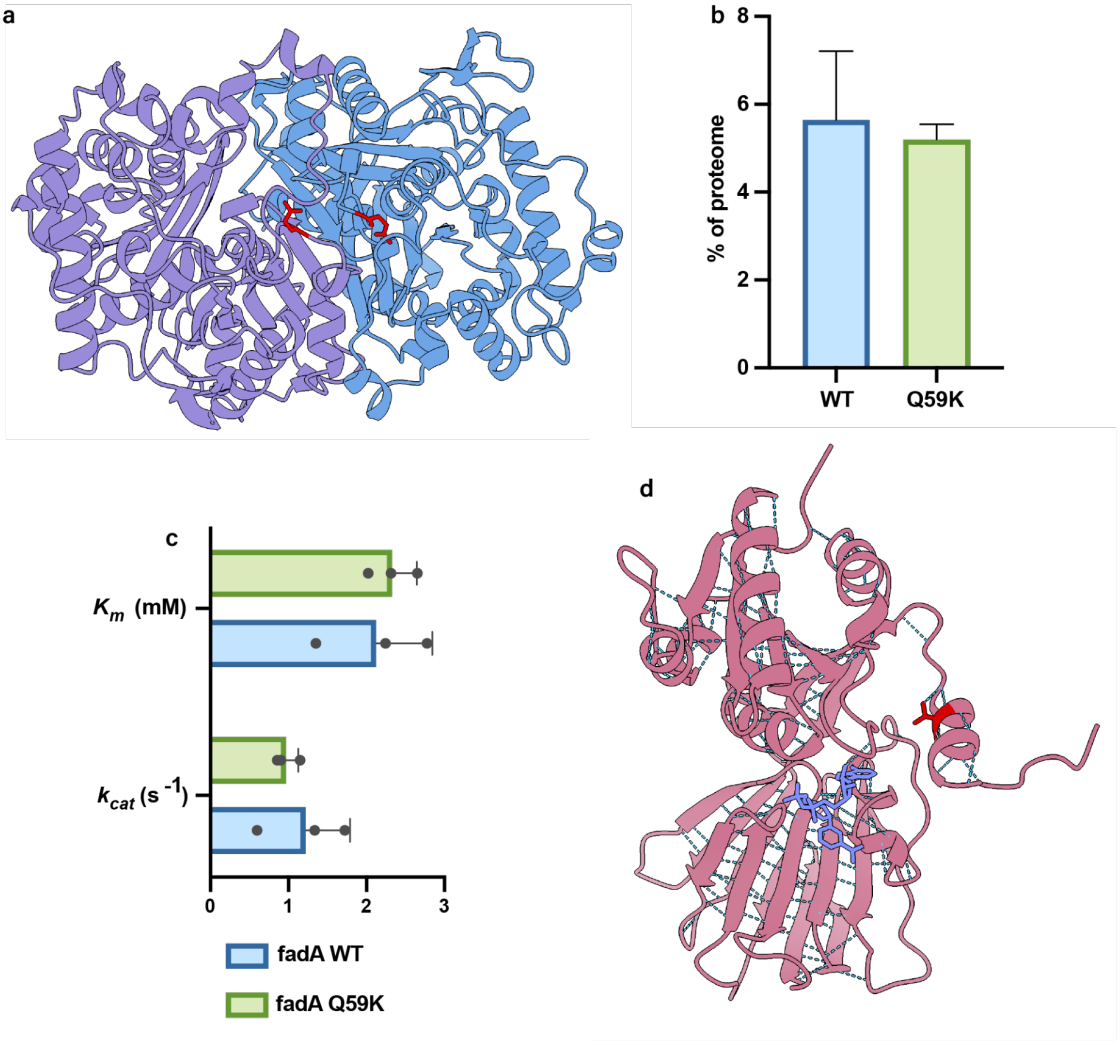

Supplementary Figure 4 Investigation of fadA and nadK mutations

a, Structural prediction of FadA homodimer (purple and blue chains) generated by Boltz-2x showing the location of Q59 in red (which was mutated to lysine in the later rounds of ALE lineage 3) at the dimer interface. **b,** Protein abundance of FadA in ALE isolates containing the WT FadA enzyme (n=24) or the mutant FadA Q59K (n=6). **c,** K_m and k_{cat} determination of FadA WT and FadA Q59K for the thiolysis reaction of acetoacetyl-CoA (n=3). **d,** Structural prediction of NadK monomer (pale pink) with NADH bound (blue) generated by Boltz-2x showing the location of T280, which mutated to alanine in later rounds of ALE lineage 1.

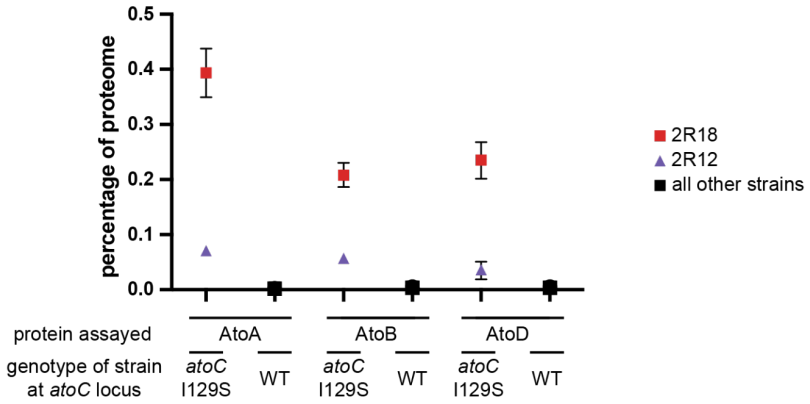

Supplementary Figure 5 Expression of proteins AtoA, AtoB and AtoD in strains containing *atoC* I129S

Expression of *ato* operon mediating short-chain fatty acid activation and β-oxidation in sequenced isolates of the ALE experiment. Expression of ato genes *atoA*, *atoB* and *atoD* is elevated in strains containing an I129S mutation to *atoC*, a characterized activator of the *ato* operon.

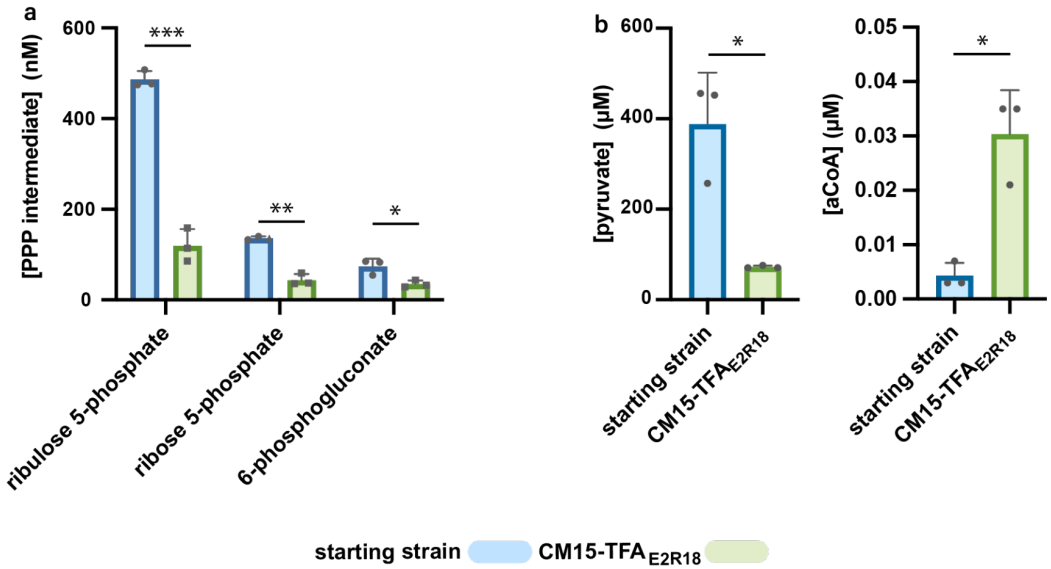

Supplementary Figure 6 Metabolomic analysis of starting and evolved CM15-TFA$_{E2R18}$ strain

a, Quantification of pentose phosphate pathway (PPP) intermediates in cell lysates showing decreased levels of ribulose 5-phosphate (p=0.0006), ribose 5-phosphate (p=0.004) and 6-phosphogluconate (p=0.03) in CM15-TFA$_{E2R18}$. **b**, Quantification of substrate and product of pyruvate formate lyase (PFL) in cell lysates showing a decreased concentration of pyruvate (p=0.04) and increased concentration of acetyl-CoA (p=0.02) in CM15-TFA$_{E2R18}$.

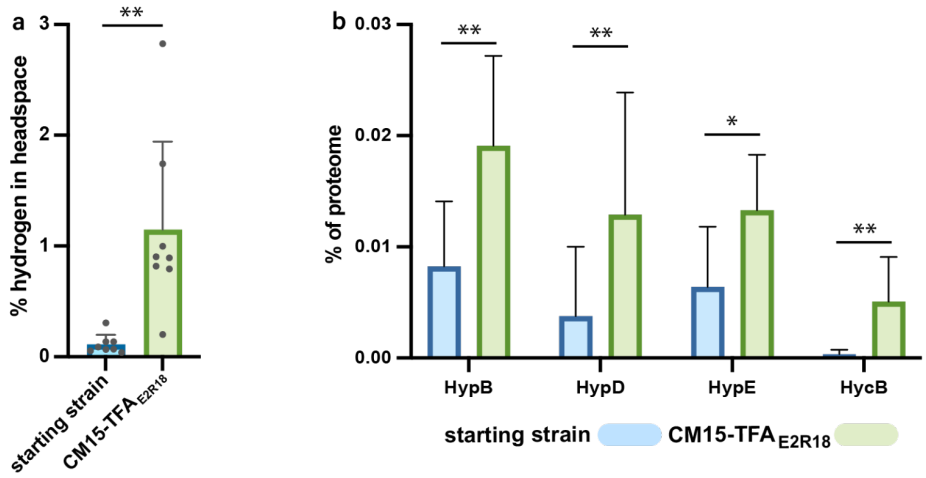

Supplementary Figure 7 Hydrogen production and hydrogenase subunit expression in the starting strain CM15-TFA and evolved strain CM15-TFA$_{E2R18}$

a, Hydrogen concentration in the headspace of sealed anaerobic vials containing cultures of CM15-TFA and evolved strain CM15-TFA$_{E2R18}$ after a 3-day fermentation (n=8). **b,** Protein abundance as the percentage of the total proteome occupied by hydrogenase maturation factors HypB/D/E and FHL subunit HycB (n=4 biological replicates assayed in triplicate).

References

1. Mehrer, C. R., Incha, M. R., Politz, M. C. & Pfleger, B. F. Anaerobic production of medium-chain fatty alcohols via a β-reduction pathway. *Metab. Eng.* **48**, 63–71 (2018).